Chapter 10
Passive Beam Combining for the Development of High Power SOA-Based Tunable Fiber Compound-Ring Lasers Using Low Power Optical Components

Muhammad A. Ummy, Simeon Bikorimana, Abdullah Hossain and Roger Dorsinville

Abstract A simple, stable, compact, and cost-effective dual-output port widely tunable SOA-based fiber compound-ring laser structure is demonstrated. Such a unique nested ring cavity enables the splitting of optical power into various branches where amplification and wavelength selection for each branch are achieved utilizing low-power SOAs and a tunable filter, respectively. Furthermore, splicing Sagnac Loop Mirrors at each end of the bidirectional fiber compound-ring cavity not only allows them to serve as variable reflectors but also enables them to channel the optical energy back to the same port thus omitting the need for high optical power combiners. Further discussed is how the said bidirectional fiber compound-ring laser structure can be extended to achieve a high-power fiber laser source by exclusively using low power optical components such as N × N couplers and (N > 1) number of SOAs. More than 98% coherent beam combining efficiency of two parallel nested fiber ring resonators is achieved over the C-band tuning range of 30 nm. Optical signal-to-noise ratio (OSNR) of +45 dB, and optical power fluctuation of less than ±0.02 dB are measured over 3 h at room temperature.

M. A. Ummy (✉)
New York City College of Technology, City University of New York, New York, USA
e-mail: maummy@citytech.cuny.edu

S. Bikorimana · A. Hossain · R. Dorsinville
The City College of New York, City University of New York, New York, USA
e-mail: sbikori00@citymail.cuny.edu

A. Hossain
e-mail: ahossai12@citymail.cuny.edu

R. Dorsinville
e-mail: rdorsinville@ccny.cuny.edu

P. Ribeiro et al. (eds.), *Optics, Photonics and Laser Technology 2017*,
Springer Series in Optical Sciences 222,
https://doi.org/10.1007/978-3-030-12692-6_10

10.1 Introduction

Extensive research has been conducted on single-mode fiber resonators of different architectures: linear [1], Fox-Smith [2], ring [3–6], and compound fiber ring [7–10] cavities. Such architectures have been established for designing and building various types of fiber laser sources with single-longitudinal mode operation for both low and high optical power applications, such as optical communication systems, scientific, medical, material processing and military purposes [11] thus underscoring the great interest in output optical power adjustability, scalability and wavelength tunability.

Wavelength selection in a fiber laser is typically achieved with different types of fiber-based optical filters. Most research works have achieved wavelength selection in a linear cavity erbium doped fiber (EDF) lasers using Fabry-Perot (FP) filters as well as Fiber Bragg Grating (FBG) based-optical filters. In addition, single longitudinal mode operation has been attained by the saturable absorption of un-pumped EDF with narrow band FBG [1]. Other architectures, such as the optical-fiber analog of Fox-Smith resonators utilize directional-coupling technologies and optical fibers to couple multiple cavities together to form compounded optical resonators resulting in several periods at the output with various modes of intensity. The highlight of this configuration is that such linked resonators can be designed to allow or suppress spectral modes, which is paramount for laser line narrowing, filtering, and spectral analysis [2].

Furthermore, equivalent phase shift (EPS) FBG filters have been used in fiber ring lasers in order to achieve ultra-narrow single transmission band selection. Typically, sampled fiber gratings (SFBGs) exhibit multiple reflection peaks when periodically changing the refractive index modulation. As previous works have demonstrated, EPS can be introduced into SFBGs by manipulating a single period out of the multiple sampling periods. This phenomenon is exploited to create an ultra-narrow single transmission band FBG filter alongside with semiconductor optical amplifiers (SOAs) as gain media (as opposed to EDFs, which suffer from wavelengths' competition and homogenous line broadening) [5]. EPS FBGs have been successfully used in several fiber-optic systems, such as distributed feedback lasers [12], optical CDMA coding [13], and single longitudinal mode fiber ring lasers [14].

Further works have improved on the ring structured EDF lasers using FBG, FP etalons and Sagnac loops to select longitudinal modes more efficiently. Single frequency and narrow line-width EDF ring lasers have been illustrated utilizing laser diodes as pumps and EDFs as gain media where fiber Faraday Rotator are introduced into the system to eliminate spatial hole burning effect [6], which can also be eliminated by the use of SOAs, for instance, in a bidirectional fiber compound-ring resonator herein discussed.

It is usually desirable to adjust and control output power of fiber lasers. Typically, complex and expensive in-line variable optical attenuators (VOA) with adjustable insertion losses are used to control the output optical power level of laser sources. Mechanical, micro-electromechanical [15–17], acousto-optic [18], electro-wetting [19], optical fiber tapers [20], and hybrid microstructure fiber-based techniques [21]

are widely used to adjust the insertion losses of the in-line fiber-based VOA. However, all-fiber based low power variable reflectors or mirrors such as SLM can also be used to adjust the optical power from both low and high-power fiber laser sources. All-single-mode fiber-based SLMs have been widely utilized in highly sensitive temperature [22], strain [23], pressure [24] sensors and wavelength optical switches [25]. Moreover, the SLMs with adjustable reflectivity have been used to form FP linear resonators [26–29] where the output optical power is dependent on the SLMs' reflectivity [30, 31]. In this work, two SLMs were utilized to regulate the optical power delivered from the two output ports of the proposed fiber compound-ring laser. Furthermore, two inexpensive low power SOAs were placed in two parallel nested ring cavities to demonstrate the possibility of achieving a highly power scalable, adjustable and switchable fiber laser structure based on multiple nested compound-ring cavities formed by N × N fiber couplers with two SLM-output couplers.

Various approaches have been employed to scale up optical power of laser sources where beam combining has shown to be a promising alternative technique of achieving high power by scaling up multiple combined laser elements. Several works have demonstrated the coupling of several anti-reflection (AR) coated laser diodes (LDs) into external cavities for operation as coherent ensembles. Placing spatial filters at the cavities' Fourier planes to serve as coherence feedback for each of the individual laser diode beams results in narrow linewidth single mode output. Contemporary research works have investigated high quality active and passive phase locking of multiple LDs using master oscillator power amplifier (MOPA) designs and optical coupling in external resonators, respectively, specifically Talbot cavities, which force collective coupled mode oscillation. The combined output power is naturally limited by the number of phase-locked LDs and their individual power. Consequently, high power laser sources with high beam quality have been demonstrated by using complex coherent and spectral beam combining techniques in external cavities [32–39]. Previous works using coherent combination techniques have illustrated the combination of several MOPAs fiber laser systems and use of single polarization low-nonlinear photonic crystal fibers to achieve relatively high combining efficiencies of up to 95% without beam quality degradation. Such works have paved the way for future works improving on brightness enhancements and increased power scalability. For instance, the use of external output coupling mirrors for coherent beam combining has been used to achieve nearly diffraction limited beam operation with significant improvement in brightness.

In addition, incoherent beam combining method [40, 41] has been used to scale up the optical power by combining individual laser elements as well. Promising results were delivered through spectral beam combination techniques by a three-channel 1-μm fiber laser with a combining efficiency of 93%. Such a system, possessing power amplifier fiber channels with a narrowband, polarized, near diffraction limited output tunable over nearly the entire 1 μm Yb^{3+} gain bandwidth, served to further heighten the prospects of increased combined beam quality, power scalability, and average power. Even improved results were obtained when four narrow linewidth Yb^{3+} doped photonic crystal fiber amplifier chains, each being of a different wavelength were combined by a polarization independent reflective diffraction grating. Michelson and

Mach-Zehnder resonators were used mostly in coherent beam combining to achieve high combining efficiency and nearly diffraction-limited beam quality [41–44]. More significantly, ring resonators have demonstrated high reliability, efficiency and stability [45] for passive coherent beam combining methods. However, achieving high power laser sources with high combining efficiency through the above approaches is not plausible without incorporating sophisticated high-power external optical components such as micro-lenses, isolators, circulators, photonic crystal fibers and MOPAs. As such, they do not serve in the interest of simplicity and cost-effectiveness. Furthermore, rare-earth, ytterbium doped fiber amplifiers (YDFAs) [45] and erbium doped fiber amplifiers (EDFAs) [46] that are usually used as gain media for beam combining to achieve high power laser systems with different types of cavity structures require external laser pumps rendering them bulky and quite inefficient. However, using nested compound-ring cavities to equally split circulating beams into N-number of low power beams for amplification by N-number of low power SOAs, one can achieve a highly efficient and high-power laser system that eliminates extra pump lasers, MOPAs, and other expensive external high power optical components.

SOAs [47], stimulated Raman scattering (SRS) amplifiers [48, 49] and stimulated Brillouin scattering (SBS) amplifiers [50, 51] have also been used as gain media in different fiber laser systems. Of all the mentioned amplifiers, SOAs stand out the most because they are more compact, light, cost effective, efficient, available for different operational regions from a wide range of wavelength spectrum, and can be incorporated into other indium phosphide (InP) based optical components. Extensive theoretical studies and analyses of SOA-based optical systems have shown that they can be used for a wide range of systems, such as, compact SOA-based laser rangefinder [52], optical pulse delay discriminator [53, 54], optical and logic gate [55] for high-speed optical communications by exploiting four-wave mixing [56, 57] and photonic integrated circuits (PIC), which provides functions for information signals imposed on optical wavelengths [58]. It must be noted that utilizing SOAs in the bidirectional fiber ring resonator structure as proposed herein eliminates the need for extra optical components such as optical isolators and circulators; thus, facilitating integration with other optical components for compact fiber laser systems. SOAs have also been used along with EDFAs to suppress optical power fluctuation in pulsed light wave frequency sweepers where the suppression of power fluctuation is attributed to the gain saturation and fast response of SOAs [59, 60].

In this work, a novel technique is proposed and validated for coherent beam combining method based on the passive phase-locking mechanism [61–63] of two C-band low power SOA-based all-single-mode fiber compound-ring resonators at 3 dB fiber couplers connecting two parallel merged ring cavities. Unlike in previous work [64], the non-adjustable multimode fiber output coupler formed by a high power and expensive power combiner with a multimode output fiber (i.e., low brightness) has been replaced by two low power SLMs to create a dual-output port all-single-mode fiber laser structure with switchable and adjustable output power. Additionally, single-mode performance is sustained to improve the brightness at the proposed fiber compound-ring laser output port. The output power of the proposed configuration was almost twice as large as the output power obtained from a single SOA-based fiber

ring or FP linear resonator [29]. More than 98% beam combining efficiency of two parallel nested fiber ring resonators is demonstrated over the C-band tuning range of 30 nm. Optical signal-to-noise ratio (OSNR) +45 dB, and optical power fluctuation of less than ±0.02 dB are measured over three hours at room temperature.

The main characteristics of the proposed fiber compound-ring laser, power tunability, and switchable output port can find applications in long-distance remote sensing [65]. Moreover, its wide range wavelength tunability can benefit various applications in fiber sensors [66–70], wavelength division multiplexer (WDM) optical communications [71], and biomedical imaging systems [72] working in the third near infrared biological window [73].

Lastly, a method to realize a highly power-scalable fiber compound-ring laser system via low power and low-cost optical components, such as tunable filters, couplers, and low power SOAs is discussed.

10.2 Experimental Setup

Figure 10.1 illustrates the experimental setup of the C-band SOA-based tunable fiber laser with two nested ring cavities (i.e., compound-ring resonator) and two broadband SLMs that can serve as either dual-output ports or a single output port depending on the reflectivity of each SLM. Each ring cavity is comprised of two branches: I-II and I-III, for the inner and the outer ring cavity, respectively. Both ring cavities share a common branch, I, which contains SOA_1 (Kamelian, OPA-20-N-C-SU), a tunable optical filter (TF-11-11-1520/1570), and a polarization controller, PC_1. Branch II contains SOA_2 (Thorlabs, S1013S), and a polarization controller, PC_2. Due to the lack of availability of a third SOA, branch III only contains a polarization controller, PC_3. As Fig. 10.1 portrays, all branches are connected by two 3 dB fiber couplers, C_1 and C_2, which are connected to SLM_1 and SLM_2, correspondingly. Each SLM (SLM_1 and SLM_2) in conjunction with a PC (PC_4 and PC_5, respectively) acts as a variable reflector. By adjusting PC_4 or PC_5, one can manipulate the reflectivity of SLM_1 and SLM_2, respectively, and switch between single and dual-output port configurations [27, 28]. Inserting the low power tunable optical filter (TF) in the common branch, I, allows wavelength selection and tuning between 1520 and 1570 nm. The three PCs (PC_1, PC_2 and PC_3) control the state of polarization of the light circulating within the compound ring cavity.

10.3 Principal of Operation

When the pump level (i.e., bias current threshold level) of either SOA is larger than the total losses of the fiber compound-ring cavity, amplified spontaneous emission (ASE) emitted from the SOAs propagates in either the forward or backward direction. For example, when a bias current, IB, of about 75 mA is injected into SOA_1 (branch I),

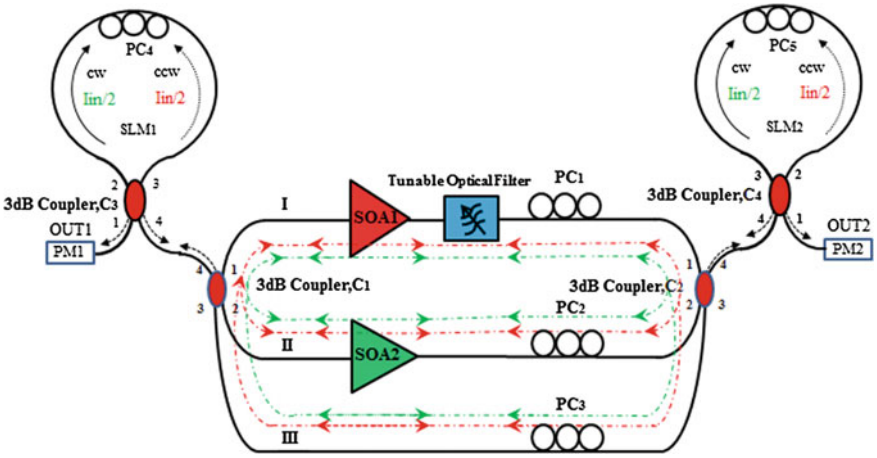

Fig. 10.1 Experimental setup of the dual SLM SOA-based TF compound-ring laser [74]

the ASE emitted by SOA_1 circulates in the clockwise (CW) direction propagating through the tunable optical filter (TF) allowing specific wavelengths to pass through polarization controller PC1 to enter port 1 of the 3 dB fiber coupler C_2 splitting the light beam equally between branches II and III at ports 2 and 3, respectively. The light beam that circulates into branch II propagates through polarization controller, PC_2, and then is amplified by SOA_2 when its bias current level, IB, is around 180 mA. This amplified light beam then reaches port 2 of 3 dB fiber coupler C_1 where it is equally divided between ports 1 and 4. Likewise, the light beam from branch III reaches port 3 after passing through polarization controller, PC_3. A half of the light beam coupled into port 1 of 3 dB fiber coupler C_1 is further amplified by SOA_1. In this fashion, a round-trip is completed in the fiber compound-ring structure, which ensures lasing. The remaining half of the light beam is coupled into output port 4 of 3 dB fiber coupler C_1 and is injected into input port 4 (i.e., I_{in}) of the SLM_1. Polarization controller, PC_4, controls the reflectivity of SLM_1 by adjusting the polarization of the light beams propagating through SLM_1. For a single output port configuration, the polarization controller, PC_4, of SLM_1 is adjusted for minimum power at output port 1 (OUT1). The counter-clockwise (CCW) and CW light beams interfere destructively and constructively at output ports 1 and 4, correspondingly of 3 dB fiber coupler, C_3, which channels the power wholly back to the compound-ring cavity.

Because the fiber compound ring resonator lacks any optical isolators within its branches, the two CCW-propagating light beams circulate in the nested ring cavities as shown in Fig. 10.1. The CCW beam from SOA_1 reaches port 1 of 3 dB coupler C_1 and splits into two equivalent light beams (i.e., 50%), which are transmitted into both ports 2 and 3. The light beam that travels into branch II is amplified by SOA_2, and passes through polarization controller PC_2 before it reaches port 2 of the 3 dB fiber coupler C_2. Similarly, the light beam that propagates through branch III passes through polarization controller PC_3 before it reaches port 3 of 3 dB fiber coupler C_2.

Half of the light beam at 3 dB fiber coupler C_2 is coupled into port 1 and propagates back into branch I to complete one round trip, while the other half of the beam is channeled into SLM_2, which then exits at output port 1 of 3 dB fiber coupler C_4 (OUT2). The output power can be controlled by polarization controller, PC_5. An optical spectrum analyzer (OSA), VOA and optical power meter (PM) were used to characterize the proposed fiber compound-ring laser. Note that the path lengths of both loops are nearly identical since all the branches have identical length and all fiber connections are done by using FC/APC connectors.

10.4 Characterization of the Fiber Compound-Ring Lasers

10.4.1 Gain Medium

The ASEs of SOA_1 and SOA_2 were characterized by using an OSA where both SOAs were set at the same bias current (I_B) of 200 mA. The ASE of both SOA_1 (green solid line) and SOA_2 (blue broken line) are shown in Fig. 10.2. Despite both SOAs being biased identically at 200 mA, they exhibited different ASE spectra. The ASE data in Fig. 10.3 indicates that SOA_1 has higher gain than SOA_2 for the same bias current level suggesting that dissimilar bias current levels are required to obtain the same output power when the SOAs are individually used in the proposed fiber compound-ring resonator.

10.4.2 Lasing Threshold Level

To determine the lasing threshold levels of the fiber compound-ring laser, the TF was set to 1550 nm and each SOA was placed individually in the proposed fiber

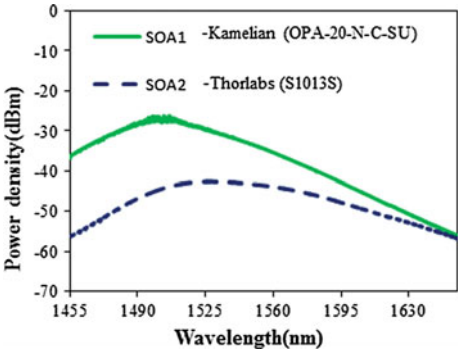

Fig. 10.2 ASE spectra of SOA_1 (green solid line) and SOA_2 (blue broken line) of the fiber compound-ring laser with both SOAs set at bias current I_B of 200 mA [74]

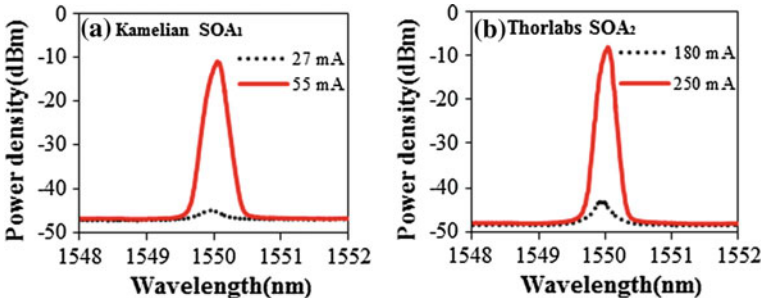

Fig. 10.3 Illustrates the output spectra of the fiber laser threshold for each individual SOA gain medium. **a** Shows the lasing threshold of SOA_1; **b** shows the lasing threshold of SOA_2 gain medium

compound-ring cavity. As shown in Fig. 10.3a and b, lasing occurs when the bias current levels of SOA_1 and SOA_2 are above the minimum threshold currents 27 mA and 180 mA respectively.

10.4.3 Tunable Optical Filter

The insertion losses (ILs) and corresponding full-width-half maximum (FWHM) linewidths within the entire tuning range (1520–1570 nm) of the tunable filter is shown in Fig. 10.4. The insertion losses decrease as the wavelength increases. The maximum and minimum ILs of 5.5 dB and 2.2 dB were measured at 1520 nm and 1570 nm, respectively. A similar downward trend was also observed when the FWHM linewidths were plotted against the wavelengths, as shown in Fig. 10.4. The linewidth varies from 0.4 to 0.32 nm at 1520 and 1570 nm, respectively.

This downward trend suggests an opposite upward trend for the output power of the proposed fiber compound-ring laser for a constant gain setting of the SOAs. It

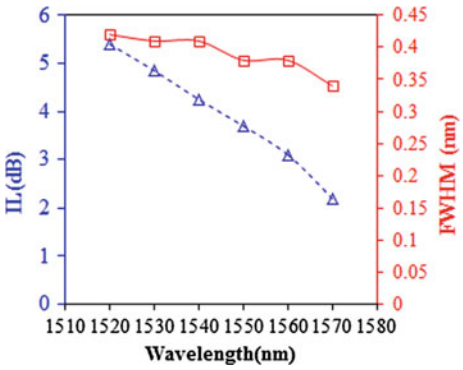

Fig. 10.4 Insertion losses (triangles), IL (dB), and FWHM (nm) (squares) spectra of the tunable optical filter [74]

Table 10.1 3 dB-Bandwidth (BW) at different bias current I_B (mA) levels and 1550 nm center wavelength with both SLMs' reflectivity set at <0.1% [74]

SOA_1 I_{B1} (mA)	SOA_2 I_{B2} (mA)	P_{OUT1} (dBm)	P_{OUT2} (dBm)	3 dB-BW (nm)
75	250	3.40	3.40	0.1985
100	300	5.80	5.70	0.2075
125	350	6.73	6.75	0.2122
150	400	7.65	7.68	0.2131
175	450	8.35	8.35	0.2157
200	500	8.94	8.95	0.2182

follows that a constant output power is achievable over the entire wavelength tuning range by adjusting the bias current (I_B) of the SOAs but at the expense of signal broadening of the fiber laser source. The reflectivity of both SLMs was set to less than 0.1% so that both output ports of the fiber compound-ring lasers (i.e., OUT1 and OUT2) have the same output power. Then, by collecting both CW and CCW light beams through SLM_1 and SLM_2, respectively, the 3 dB bandwidth was measured at different bias current levels at 1550 nm wavelength by using an OSA. The 3 dB-bandwidth increased from 0.1985 to 0.2182 nm as the bias current was increased to the standard bias current of each of the SOAs (see Table 10.1).

10.4.4 Coherent Beam Combining Efficiency

The principle of the proposed passive coherent beam combining technique of dual compound-ring based fiber lasers with two adjustable output couplers (i.e., SLMs) is based on the passive phase-locking mechanism caused by spontaneous self-organization operation [58, 60]. The wide bandwidth of the SOAs facilitates the passive phase-locking mechanism, thus allowing the fields' self-adjustment to select common oscillating modes or resonant frequencies of the counter-propagating (i.e., clockwise and counter-clockwise) light beams in the two merged ring cavities and optimize their in-phase locking state conditions without any active phase-locking systems.

To assess the beam combining efficiency of the proposed fiber laser structure, utilized each individual SOA was utilized as a gain medium in the common branch, I, of the compound-ring cavity and measured the output power at both its output couplers: OUT1 and OUT2. Following that, both SOAs were placed simultaneously within the compound-ring cavities (branches I and II, respectively) and measured the output power at both output couplers. Note that the SLMs' reflectivity was adjusted to the maximum (i.e. >99.9%) and minimum (i.e., <0.1%), respectively. The tunable filter was manually adjusted from 1535 to 1565 nm and each SOA was driven and kept constant at its standard bias current, 200 and 500 mA, respectively. Figure 10.5 illustrates the passive coherent beam combining efficiency spectrum (right vertical

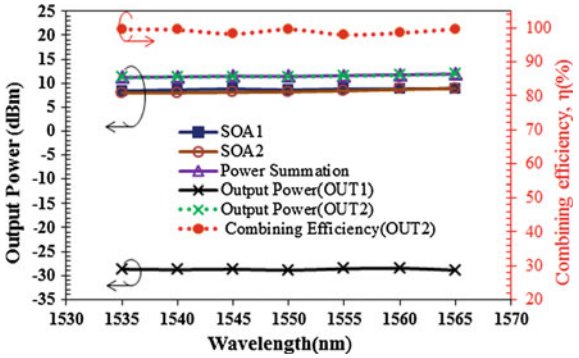

Fig. 10.5 Output power and combining efficiency spectra of the proposed dual-SLM SOA-based tunable fiber compound-ring laser system using two SOAs as gain media. Individual SOA output power spectrum: SOA_1 (filled squares), SOA_2 (unfilled circles), output power summation spectrum of both SOAs (unfilled triangles), and actual measured output power (crosses) at the output port, OUT2 with SOA_1 and SOA_2 driven at 200 mA and 500 mA constant bias current. The PC_1 and PC_2 were maximized for each wavelength [71]

axis) and the output power spectrum (left vertical axis) from the proposed fiber compound-ring laser operating with the individual SOAs as well as both SOAs over the C-band tuning range of 30 nm.

The beam combining efficiency (filled circles) was obtained by dividing the optical power measured at the output port (OUT2) under dual SOA fiber laser operation by the power summation (unfilled triangles) of the same port under individual SOA operation: SOA_1 (filled squares) and SOA_2 (unfilled circles) (i.e., $\eta = [P_{measured}/(P_{SOA1} + P_{SOA2})]$. The leakage optical power spectrum (unfilled squares) at the other output port (OUT_1) re-mained below −28.5 dBm. The maximum output power delivered with SOA_1 (Kamelian model) and SOA_2 (Thorlabs model) separately was +8.91 and +8.90 dBm at 1565 nm. On the other hand, when both SOAs were placed in the compound-ring cavities, the maximum measured output power obtained at the output port, OUT2, was +11.9 dBm at 1565 nm, which was double of that obtained with just either SOA. The maximum output power obtained by adding the optical power from a single SOA versus dual SOA fiber laser operation at the output port, OUT2, both at 1565 nm, was +11.91 dBm and +11.9 dBm, respectively. This is where the insertion losses of the tunable filter were the lowest.

The maximum and minimum obtained combining efficiencies (filled circles) were 99.76% and 98.06% at 1565 nm and 1555 nm, respectively, as shown in Fig. 10.5 (right vertical axis).

10.4.5 Fiber Laser Power Tunability and Its Switchable Dual-Output Port Operation

The proposed fiber compound-ring laser can operate with two adjustable and switchable output ports (i.e., OUT1 and OUT2). The output power from either output port can be tuned by simply controlling the bias current levels and thus gain levels of the SOAs or by adjusting the reflectivity of the SLMs while keeping the former constant.

The SOA gain was adjusted by setting the tunable filter at 1550 nm wavelength and adjusting the bias current levels of the SOAs. Table 10.2 shows the output power evolution at both output ports, OUT1 and OUT2 as a function of the bias current levels, I_{B1} and I_{B2}. The reflectivity of SLM_1 and SLM_2 was set to $\geq$99.9% and $\leq$0.1%, respectively. The achieved maximum dynamic range was 40.75 dB at 1550 nm wavelength and standard bias current levels of 200 and 500 mA for SOA_1 and SOA_2, respectively.

The second approach involves adjusting the reflectivity of both SLM_1 and SLM_2 while keeping the gain of the SOAs constant (i.e., I_{B1} and I_{B2} is fixed at 200 and 500 mA, respectively). Depending on the reflectivity of SLM1 and SLM_2, the proposed fiber compound-ring laser can be operated as either a single or a dual-output configuration.

In a single output configuration, one of the SLMs, either SLM_1 or SLM_2, should be kept at the highest reflectivity (i.e., $\geq$99.9%) while the other should be set to its lowest reflectivity of (i.e., $\geq$0. 1%). For us to characterize the power tunability performance of both output ports of the fiber laser, the tunable filter was to 1550 nm, and initialized the reflectivity settings of SLM_1 and SLM_2 to $\leq$0.1% and $\geq$99.9%, respectively as explained earlier. The initial measured output power from both output ports, OUT1 and OUT2 was +11.85 dBm and −28.9 dBm, respectively. The reflectivity of SLM_1 was gradually changed by slowly adjusting polarization controller PC_4, while recording the power meter readings and the output signal spectrum at both output ports, OUT1 and OUT2, and the FWHM at output port, OUT1. The output power from output port OUT1, was thus changed from +11.85 to −28.5 dBm while maintaining the output power at output port OUT2 at −28.9 dBm by adjusting polarization controller PC_5 for SLM_2. The above process was then reversed by

Table 10.2 Optical power from the fiber laser output-port, OUT1 AND OUT2, at different bias current I_B (mA) levels and 1550 nm center wavelength

SOA_1 I_{B1} (mA)	SOA_2 I_{B2} (mA)	P_{OUT1} (dBm)	P_{OUT2} (dBm)
26	180	−36	−1.5
50	200	−32	5
75	250	−29.5	7.8
100	300	−28.9	9.3
150	400	−28.6	11.1
200	500	−28.9	11.85

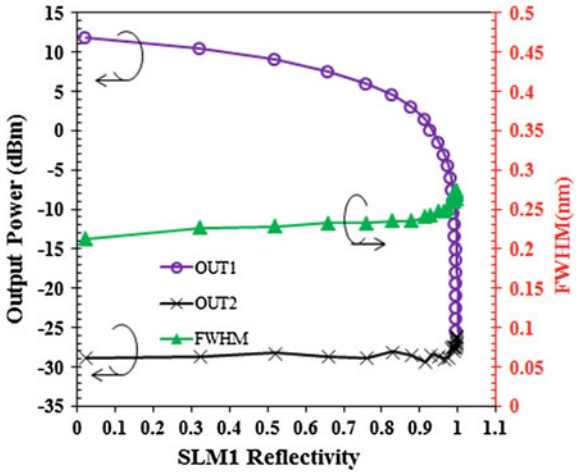

Fig. 10.6 Shows the output power of output port, OUT1 (circles) and OUT2 (crosses), respectively, and the 3 dB-bandwidth of output port, OUT1 (tringles) as a function of different reflectivity values of the Sagnac loop mirror, SML_1 for single output port operation

switching the reflectivity of SLM_1 and SLM_2 to $\geq$99.9% and $\leq$0.1%, respectively and examining the ports' performances as done above. In this case, the measured output power from output port, OUT2 was adjusted from +11.87 to −28.9 dBm while maintaining the output port, OUT1, at −28.9 dBm. Figure 10.6 illustrates the output power from both output ports, OUT1 (circles) and OUT2 (crosses) as a function of the reflectivity of SLM_1. Note that both output ports behave similarly and that the 3 dB-bandwidth of the light beam from OUT1 (triangles) increased as the reflectivity of the SLM_1 increased while the output power decreased due to strong feedback (i.e., reflected light beam) from each of the SLMs.

In the dual-output port configuration, both output ports can be fixed and adjusted to any output power level between +11.9 and −28.9 dBm. As portrayed in Fig. 10.7, both output ports, OUT1 and OUT2, were set to +8.94 and +8.95 dBm, respectively by adjusting the reflectivity of both SLM_1 and SLM_2 to $\leq$0.1%. Then, the output power from output port OUT1, was gradually tweaked from +8.94 to −28.9 dBm by adjusting the reflectivity of the SLM_1 from 0.1% to more than 99.9% while simultaneously optimizing the reflectivity of SLM_2 to keep the output power at OUT2 constant at +8.95 dBm. The reflectivity of SLM_2 was around 50% while that of SLM_1 was around 99.9% for the output power at OUT2 constant at +8.95 dBm.

10.4.6 Wavelength Tunability

The wavelength tuning width of the optical filter is 50 nm (see Fig. 10.4); its maximum IL, 5.5 dB, occurs at 1520 nm while its minimum IL, 2.2 dB, occurs at 1570 nm. The bias currents for SOA_1 and SOA_2 was set at 200 and 500 mA, respectively. Then the reflectivity of SLM_1 and SLM_2 was adjusted and set constant at $\leq$0.1% and $\geq$99.9%, respectively. Then by optimizing the polarization controllers, PC_1, PC_2 and PC_3 as

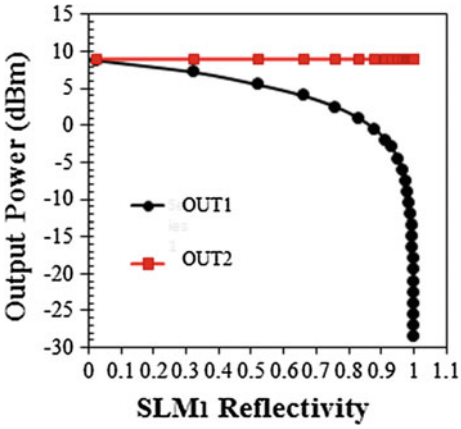

Fig. 10.7 Illustrates the output power from both output ports, OUT1 (filled circles) and OUT2 (unfilled squares) for different reflectivity values of the Sagnac loop mirror, SLM_1 for dual-output port operation while maintaining constant output power at OUT2 constant at +8.95 dBm [74]

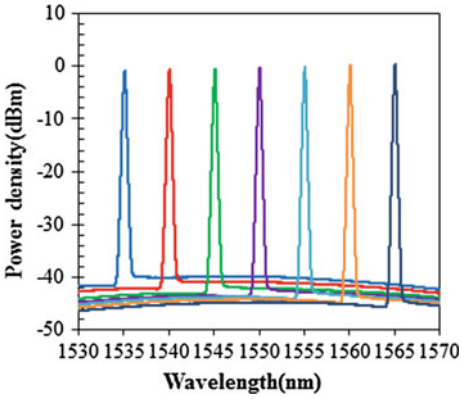

Fig. 10.8 Shows the wavelength spectrum of the fiber compound-ring laser where PC_1, PC_2 and PC_3, were optimized at each wavelength [74]

the TF was set to 1535, 1540, 1545, 1550, 1555, 1560 and 1565 nm, the output light beam was measured as expressed in Fig. 10.8.

10.4.7 Optical Signal-to-Noise Ratio

The peak signals measured by the OSA within the wavelength spectrum in question (see Fig. 10.8) were used to calculate the optical signal-to-noise ratio (OSNR) of system by subtracting the peak power value at each center wavelength (i.e., 1535, 1540, 1545, 1550, 1555, 1560 and 1565 nm) from the background noise level of each wavelength spectrum (i.e., $OSNR(dB) = P_{Signal} - P_{Noise}$, where both P_{Signal} and P_{Noise} level are expressed in dBm), as demonstrated in Fig. 10.9. The OSNR remained well above +39 dB over the whole wavelength tuning range in which the maximum OSNR of +44.6 dB was found to be at 1565 nm.

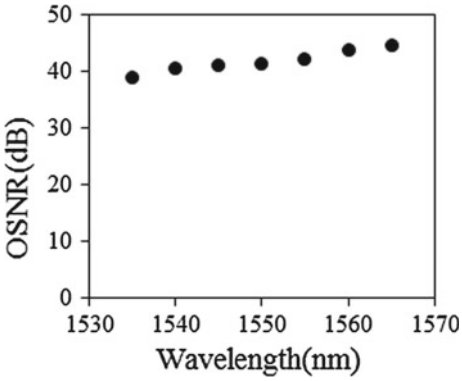

Fig. 10.9 Shows the OSNR at each center wavelength spectrum, 1535, 1540, 1545, 1550, 1550, 1555, 1560 and 1565 nm with optimized PC_1, PC_2 and PC_3

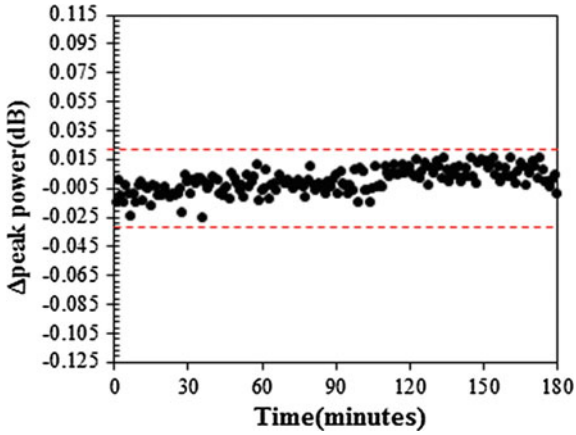

Fig. 10.10 Shows the output power short-term fluctuations of the proposed fiber compound-ring laser at 1550 nm wavelength

The obtained OSNR spectrum of our fiber compound ring laser is comparable to that of those used in remote sensing [75, 76], fiber sensors that utilize wavelength-peak measurement method [67] and optical communication systems [77].

10.4.8 Short-Term Optical Power

Lastly, using the OSA to monitor results and acquire data, the short-term optical power stability test was conducted at room temperature with the SOAs set to their standard bias current levels and the tunable filter fixed at 1550 nm central wavelength. The optical stability test was carried out over a total duration of 180 min with 1 min intervals and an OSA resolution bandwidth of 0.01 nm without additional data averaging. Figure 10.10 demonstrates that the proposed fiber compound-ring laser, whose power fluctuations were within ±0.02 dB and could have been further reduced by proper packaging of the system, is very stable.

10.5 (N ≫ 1) SOAs Based Fiber Compound-Ring Laser Structure

Thus far, the high passive coherent beam combining efficiency of two SOAs based fiber compound-ring laser without the use of active phase modulators has been successfully demonstrated. The proposed fiber compound-ring cavity has high prospects to realize an efficient, stable, simple, low-cost, compact, and highly power-scalable fiber system by passively combining [53, 54] low power (N ≫ 1) number of SOAs fiber compound-ring lasers by using N × N fiber couplers with high beam combining efficiency. Estimation studies have shown that the beam combining efficiency worsens with a higher number (i.e. N > 8) [78] of individual combined Y-shaped linear cavity based fiber lasers. Yet as demonstrated in other works [79], several individual fiber lasers have been combined in Y-shape coupled arrays with high efficient coherent beam combining from 16 channels designed by cascading two fiber laser arrays using EDFAs as gain media. Thus, in addition to cascading multiple arrays of compound-ring laser cavities for the proposed (N ≫ 1) fiber laser compound-ring laser, one can also utilize SOAs because of their wide bandwidths, which enable sufficient lasing modes within the actual gain bandwidth. Yet, it is expected that the changes in the behavior of mode competition among the oscillating modes will potentially diminish the likelihood of obtaining the same spectral lasing mode [80, 81] thus degrading the beam combining efficiency when many arrays of merged compound-ring resonators are combined. In addition, the nonlinearities, optical damages and nonlinear effects (SRS, SBS, and four-wave mixing in all-single-mode fiber output couplers) that manifest in a SOA [82] at very high optical power will restrict the maximum amount of achievable optical power from the proposed fiber compound-ring laser.

This work has enhanced and improved on previous works [55] by omitting the expensive high-power combiner with a multimode fiber output port. The proposed SOA-based fiber compound-ring laser structure is a dual-output port all-single-mode-fiber laser structure that can be used in single or dual-output operation with adjustable output power. Figure 10.11 illustrates the proposed fiber laser structure with NxN fiber couplers and two SLMs, SLM_1 and SLM_2, which form the output couplers, OUT1 and OUT2.

10.6 Conclusion

Various work and advancements have been realized leading up to and paving the way the for further research on SOA based-fiber laser sources, which can increasingly be established in current optical applications due to their compact, cost effective, and user-friendly nature as opposed to their counterparts that utilize rare-earth YDFAs, EDFAs, SRS amplifiers, SBS amplifiers as well as free-space solid state laser sources. Newer designs aim to eliminate the bulkiness of conventional fiber laser systems

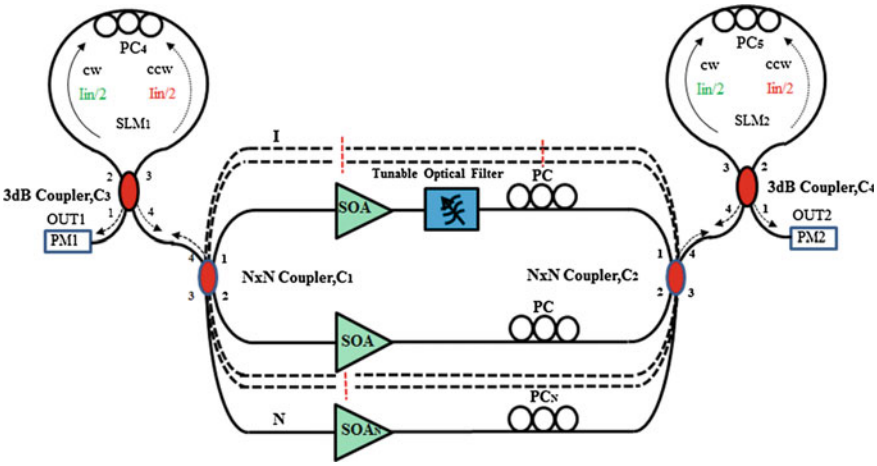

Fig. 10.11 (N ≫ 1) number of SOAs based dual-output port fiber compound-ring laser structure

as discussed earlier by obsoleting optical isolators and circulators thus, paving the avenue for the fabrication of a simple, on-chip scalable, power scalable, adjustable and switchable laser source.

To this end, a dual-SOA based all-single-mode dual parallel nested fiber ring resonator with two SLMs (to enable operational mode switching and output power adjustability thus bypassing the need for VOAs) was designed, which resulted in an impressive coherent beam combining efficiency of 98% over the C-band tuning range of 30 nm, optical signal-to -noise ratio (OSNR) of +45 dB, and optical power fluctuation within 0.02 dB over the course of 3 h at room temperature.

The chapter then concluded by discussing using N × N fused fiber couplers to achieve an all-single-mode-fiber compound-ring laser structure with (N ≫ 1) number of SOAs for power scaling to design a high-power laser source using low power optical components exclusively. Due to the advanced technologies of SOAs and tunable filters covering a wide range of wavelength spectrum in different electromagnetic spectrum bands, the proposed fiber compound-ring laser can be used to build compact laser systems covering different optical wavelength-bands as well.

References

1. X. He, X. Fang, C. Liao, D.N. Wang, J. Sun, A tunable and switchable single-longitudinal-mode dual-wavelength fiber laser with a simple linear cavity. Opt. Express **17**, 21773–21781 (2009)
2. P. Barnsley, P. Urquhart, C. Millar, M. Brierley, Fiber Fox-Smith resonators: application to single-longitudinal-mode operation of fiber lasers. J. Opt. Soc. Am. A **5**, 1339–1346 (1988)
3. K. Iwatsuki, A. Takada, K. Hagimoto, M. Saruwatari, Y. Kimura, M. Shimizu, Er3+-doped fiber-ring-laser with less than 10 kHz linewidth, in *Optical Fiber Communication Conference,*

Vol. 5 of 1989 OSA Technical Digest Series (Optical Society of America, 1989), paper PD5
4. J. Zhang, C.Y. Yue, G.W. Schinn, W.R.L. Clements, J.W.Y. Lit, Stable single-mode compound-ring erbium-doped fiber laser. J. Lightwave Technol. **14**, 104–109 (1996)
5. X. Chen, J. Yao, Z. Deng, Ultranarrow dual-transmission-band fiber Bragg grating filter and its application in a dual-wavelength single-longitudinal-mode fiber ring laser. Opt. Lett. **30**, 2068–2070 (2005)
6. Z. Ou, Z. Dai, B. Wu, L. Zhang, Z. Peng, Y. Liu, Research of narrow line-width Er3+-doped fiber ring laser with FBG F-P etalon and FBG Sagnac loop, in *Microelectronic and Optoelectronic Devices and Integration, 2009 International Conference on Optical Instruments and Technology 2008*
7. J. Zhang, J.W.Y. Lit, Compound fiber ring resonator: theory. J. Opt. Soc. Am. A **11**, 1867–1873 (1994)
8. P. Urquhart, Compound optical-fiber-based resonators. J. Opt. Soc. Am. A **5**, 803–812 (1988)
9. J. Zhang, J.W.Y. Lit, All-fiber compound ring resonator with a ring filter. J. Lightwave Technol. **12**, 1256–1262 (1994)
10. J. Capmany, M.A. Muriel, A new transfer matrix formalism for the analysis of fiber ring resonators: compound coupled structures for FDMA demultiplexing. J. Lightwave Technol. **8**, 1904–1919 (1990)
11. W. Shi, Q. Fang, X. Zhu, R.A. Norwood, N. Peyghambarian, Fiber lasers and their applications [Invited]. Appl. Opt. **53**, 6554–6568 (2014)
12. D.J. Jiang, X.F. Chen, Y.T. Dai, H.T. Liu, S.Z. Xie, A novel distributed feedback fiber laser based on equivalent phase shift. IEEE Photon. Technol. Lett. **16**, 2598 (2004)
13. Y.T. Dai, X.F. Chen, D.J. Jiang, S.Z. Xie, C.C. Fan, Equivalent phase shift in a fiber Bragg grating achieved by changing the sampling period. IEEE Photon. Technol. Lett. **16**, 2284 (2004)
14. X.F. Chen, J.P. Yao, F. Zeng, Z.C. Deng, Single-longitudinal-mode fiber ring laser employing an equivalent phase-shifted fiber Bragg grating. IEEE Photon. Technol. Lett. **17**, 1390 (2004)
15. R.R.A. Syms, H. Zou, J. Stagg, H. Veladi, Sliding-blade MEMS iris and variable optical attenuator. J. Micromech. Microeng. **14**, 1700 (2004)
16. A. Unamuno, D. Uttamchandani, MEMS variable optical attenuator with Vernier latching mechanism. IEEE Photon. Technol. Lett. **18**, 88–90 (2006)
17. C. Marxer, P. Griss, N.F. de Rooij, A variable optical attenuator based on silicon micromechanics. IEEE Photon. Technol. Lett. **11**, 233–235 (1999)
18. Q. Li, A.A. Au, C.-H. Lin, E.R. Lyons, H.P. Lee, An efficient all-fiber variable optical attenuator via acoustooptic mode coupling. IEEE Photon. Technol. Lett. **14**, 1563–1565 (2002)
19. A. Duduś, R. Blue, M. Zagnoni, G. Stewart, D. Uttamchandani, Modeling and characterization of an electrowetting-based single-mode fiber variable optical attenuator. IEEE J. Sel. Topics Quantum Electron. **21**, 253–261 (2015)
20. A. Benner, H.M. Presby, N. Amitay, Low-reflectivity in-line variable attenuator utilizing optical fiber tapers. J. Lightwave Technol. **8**, 7–10 (1990)
21. C. Kerbage, A. Hale, A. Yablon, R.S. Windeler, B.J. Eggleton, Integrated all-fiber variable attenuator based on hybrid microstructure fiber. Appl. Phys. Lett. **79**, 3191–3193 (2001)
22. K.S. Lim, C.H. Pua, S.W. Harun, H. Ahmad, Temperature-sensitive dual-segment polarization maintaining fiber Sagnac loop mirror. Opt. Laser Technol. **42**, 377–381 (2010)
23. G. Sun, D.S. Moon, Y. Chung, Simultaneous temperature and strain measurement using two types of high-birefringence fibers in Sagnac loop mirror. IEEE Photon. Technol. Lett. **19**, 2027–2029 (2007)
24. H.Y. Fu, H.Y. Tam, L.-Y. Shao, X. Dong, P.K.A. Wai, C. Lu, S.K. Khijwania, Pressure sensor realized with polarization-maintaining photonic crystal fiber-based Sagnac interferometer. Appl. Opt. **47**, 2835–2839 (2008)
25. G. Das, J.W.Y. Lit, Wavelength switching of a fiber laser with a Sagnac loop reflector. IEEE Photon. Technol. Lett. **16**, 60–62 (2004)
26. D.S. Lim, H.K. Lee, K.H. Kim, S.B. Kang, J.T. Ahn, M.Y. Jeon, Generation of multiorder Stokes and anti-Stokes lines in a Brillouin erbium-fiber laser with a Sagnac loop mirror. Opt. Lett. **23**, 1671–1673 (1998)

27. S.S. Wang, Z.F. Hu, Y.H. Li, L.M. Tong, All-fiber Fabry-Perot resonators based on microfiber Sagnac loop mirrors. Opt. Lett. **34**, 253–255 (2009)
28. M.A. Ummy, N. Madamopoulos, P. Lama, R. Dorsinville, Dual Sagnac loop mirror SOA-based widely tunable dual-output port fiber laser. Opt. Express **17**, 14495–14501 (2009)
29. M.A. Ummy, N. Madamopoulos, A. Joyo, M. Kouar, R. Dorsinville, Tunable multi-wavelength SOA based linear cavity dual-output port fiber laser using Lyot-Sagnac loop mirror. Opt. Express **19**, 3202–3211 (2011)
30. D.B. Mortimore, Fiber loop reflectors. J. of Lightwave Technol. **6**, 1217–1224 (1988)
31. S. Feng, Q. Mao, L. Shang, J.W. Lit, Reflectivity characteristics of the fiber loop mirror with a polarization controller. Opt. Commun. **277**, 322–328 (2007)
32. S. Klingebiel, F. Röser, B. Ortaç, J. Limpert, A. Tünnermann, Spectral beam combining of Yb-doped fiber lasers with high efficiency. J. Opt. Soc. Am. B **24**, 1716–1720 (2007)
33. V. Raab, R. Menzel, External resonator design for high-power laser diodes that yields 400 mW of TEM_{00} power. Opt. Lett. **27**, 167–169 (2002)
34. C.J. Corcoran, R.H. Rediker, Operation of five individual diode lasers as a coherent ensemble by fiber coupling into an external cavity. Appl. Phys. Lett. **59**, 759–761 (1991)
35. B. Liu, Y. Braiman, Coherent beam combining of high power broad-area laser diode array with near diffraction limited beam quality and high power conversion efficiency. Opt. Express **21**, 31218–31228 (2013)
36. V. Daneu, A. Sanchez, T.Y. Fan, H.K. Choi, G.W. Turner, C.C. Cook, Spectral beam combining of a broad-stripe diode laser array in an external cavity. Opt. Lett. **25**, 405–407 (2000)
37. T.H. Loftus, A. Liu, P.R. Hoffman, A.M. Thomas, M. Norsen, R. Royse, E. Honea, 522 W average power, spectrally beam-combined fiber laser with near-diffraction-limited beam quality. Opt. Lett. **32**, 349–351 (2007)
38. T.Y. Fan, Laser beam combining for high-power, high-radiance sources. IEEE J. Sel. Topics Quantum Electron. **11**, 567–577 (2005)
39. S.J. Augst, A.K. Goyal, R.L. Aggarwal, T.Y. Fan, A. Sanchez, Wavelength beam combining of ytterbium fiber lasers. Opt. Lett. **28**, 331–333 (2003)
40. C. Wirth, O. Schmidt, I. Tsybin, T. Schreiber, T. Peschel, F. Brückner, T. Clausnitzer, J. Limpert, R. Eberhardt, A. Tünnermann, M. Gowin, E.T. Have, K. Ludewigt, M. Jung, 2 kW incoherent beam combining of four narrow-linewidth photonic crystal fiber amplifiers. Opt. Express **17**, 1178–1183 (2009)
41. P. Sprangle, A. Ting, J. Penano, R. Fischer, B. Hafizi, Incoherent combining and atmospheric propagation of high-power fiber lasers for directed-energy applications. IEEE J. Quantum Electron. **45**, 138–148 (2009)
42. D. Sabourdy, V. Kermène, A. Desfarges-Berthelemot, M. Vampouille, A. Barthélémy, Coherent combining of two Nd: YAG lasers in a Vernier–Michelson-type cavity. Appl. Phys. B **75**, 503–507 (2002)
43. G. Bloom, C. Larat, E. Lallier, M. Carras, X. Marcadet, Coherent combining of two quantum-cascade lasers in a Michelson cavity. Opt. Lett. **35**, 1917–1919 (2010)
44. D. Sabourdy, V. Kermène, A. Desfarges-Berthelemot, L. Lefort, A. Barthélémy, P. Even, D. Pureur, Efficient coherent combining of widely tunable fiber lasers. Opt. Express **11**, 87–97 (2003)
45. F. Jeux, A. Desfarges-Berthelemot, V. Kermène, A. Barthelemy, Experimental demonstration of passive coherent combining of fiber lasers by phase contrast filtering. Opt. Express **20**, 28941–28946 (2012)
46. V.A. Kozlov, J. Hernández-Cordero, T.F. Morse, All-fiber coherent beam combining of fiber lasers. Opt. Lett. **24**, 1814–1816 (1999)
47. D.S. Moon, B.H. Kim, A. Lin, G. Sun, W.T. Han, Y.G. Han, Y. Chung, Tunable multi-wavelength SOA fiber laser based on a Sagnac loop mirror using an elliptical core side-hole fiber. Opt. Express **15**, 8371–8376 (2007)
48. C.S. Kim, R.M. Sova, J.U. Kang, Tunable multi-wavelength all-fiber Raman source using fiber Sagnac loop filter. Opt. Commun. **218**, 291–295 (2003)

49. P.G. Zverev, T.T. Basiev, A.M. Prokhorov, Stimulated Raman scattering of laser radiation in Raman crystals. Opt. Mater. **11**, 335–352 (1999)
50. S.P. Smith, F. Zarinetchi, S. Ezekiel, Narrow-linewidth stimulated Brillouin fiber laser and applications. Opt. Lett. **16**, 393–395 (1991)
51. J.C. Yong, L. Thévenaz, B. Yoon Kim, Brillouin fiber laser pumped by a DFB laser diode. J. Lightwave Technol. **21**, 546 (2003)
52. A.J. Lowery, M. Premaratne, Design and simulation of a simple laser rangefinder using a semiconductor optical amplifier-detector. Opt. Express **13**, 3647–3652 (2005)
53. A.J. Lowery, M. Premaratne, Reduced component count optical delay discriminator using a semiconductor optical amplifier-detector. Opt. Express **13**, 290–295 (2005)
54. M. Premaratne, A.J. Lowery, Analytical characterization of SOA-based optical pulse delay discriminator. J. Lightwave Technol. **23**, 2778–2787 (2005)
55. N. Arez, M. Razaghi, Optical and logic gate implementation using four wave mixing in semiconductor optical amplifier for high speed optical communication systems, in *International Conference Network and Electronics Engineering (IPCSIT), 2011*, vol. 11
56. N. Das, M. Razaghi, R. Hosseini, Four-wave mixing in semiconductor optical amplifiers for high-speed communications, in *2012 5th International Conference on Computers and Devices for Communication (CODEC)*, IEEE (2012)
57. N.K. Das, Y. Yamayoshi, H. Kawaguchi, Analysis of basic four-wave mixing characteristics in a semiconductor optical amplifier by the finite-difference beam propagation method. IEEE J. Quantum Electron. **36**, 1184–1192 (2000)
58. H. Heidrich, Multifunctional photonic integrated circuits based on SOA and ring resonators, in *Optical Fiber Communication Conference, Vol. 1 of 2003 OSA Technical Digest Series (Optical Society of America, 2003), paper TuG3*
59. K. Sato, H. Toba, Reduction of mode partition noise by using semiconductor optical amplifiers. IEEE J. Sel. Topics Quantum Electron. **7**, 328–333 (2001)
60. K. Takano, K. Nakagawa, Y. Takahashi, H. Ito, Reduction of power fluctuation in pulsed lightwave frequency sweepers with SOA following EDFA. IEEE Photon. Technol. Lett. **19**, 525–527 (2007)
61. H. Bruesselbach, D.C. Jones, M.S. Mangir, M. Minden, J.L. Rogers, Self-organized coherence in fiber laser arrays. Opt. Lett. **30**, 1339–1341 (2005)
62. J. Lhermite, A. Desfarges-Berthelemot, V. Kermene, A. Barthelemy, Passive phase locking of an array of four fiber amplifiers by an all-optical feedback loop. Opt. Lett. **32**, 1842–1844 (2007)
63. B. Lei, Y. Feng, Phase locking of an array of three fiber lasers by an all-fiber coupling loop. Opt. Express **15**, 17114–17119 (2007)
64. M.A. Ummy, S. Bikorimana, N. Madamopoulos, R. Dorsinville, Beam combining of SOA-based bidirectional tunable fiber nested ring lasers with continuous tunability over the C-band at room temperature. J. Lightwave Technol. **34**, 3703–3710 (2016)
65. J.P. Cariou, B. Augere, M. Valla, Laser source requirements for coherent lidars based on fiber technology. ComptesRendus Phys. **7**, 213–223 (2006)
66. A. Martinez-Ríos, G. Anzueto-Sanchez, R. Selvas-Aguilar, A.A.C. Guzman, D. Toral-Acosta, V. Guzman-Ramos, V.M. Duran-Ramirez, J.A. Guerrero-Viramontes, C.A. Calles-Arriaga, High sensitivity fiber laser temperature sensor. IEEE Sensors J. **5**, 2399–2402 (2015)
67. T.B. Pham, H. Bui, H.T. Le, V.H. Pham, Characteristics of the fiber laser sensor system based on etched-Bragg grating sensing probe for determination of the low nitrate concentration in water. Sensors **17**, 7 (2016)
68. H. Fu, D. Chen, Z. Cai, Fiber sensor systems based on fiber laser and microwave photonic technologies. Sensors **12**, 5395–5419 (2012)
69. N.S. Park, S.K. Chun, G.H. Han, C.S. Kim, Acousto-optic-based wavelength-comb-swept laser for extended displacement measurements. Sensors **17**, 740 (2017)
70. P.C. Peng, J.H. Lin, H.Y. Tseng, S. Chi, Intensity and wavelength-division multiplexing FBG sensor system using a tunable multiport fiber ring laser. IEEE Photon. Technol. Lett. **16**, 230–232 (2004)

71. F. Delorme, Widely tunable 1.55 μm lasers for wavelength-division-multiplexed optical fiber communications. IEEE J. Sel. Topics Quantum Electron. **34**, 1706–1716 (1998)
72. S.H. Yun, G.J. Tearney, J.F. de Boer, N. Iftimia, B.E. Bouma, High-speed optical frequency-domain imaging. Opt. Express **11**, 2953–2963 (2003)
73. E. Hemmer, A. Benayas, F. Légaré, F. Vetrone, Exploiting the biological windows: current perspectives on fluorescent bioprobes emitting above 1000 nm. Nanoscale Horiz. **1**, 168–184 (2016)
74. M.A. Ummy, S. Bikorimana, R. Dorsinville, Beam combining of SOA-based bidirectional tunable fiber compound-ring lasers with external reflectors, in *Optics and Lasers Technology, 2017 5th International Conference on Photonics. PHOTOPTICS, 2017*
75. G. Wang, L. Zhan, J. Liu, T. Zhang, J. Li, L. Zhang, J. Peng, L. Yi, Watt-level ultrahigh-optical signal-to-noise ratio single-longitudinal-mode tunable Brillouin fiber laser. Opt. Lett. **38**, 19–21 (2013)
76. Y. Luo, Y. Tang, J. Yang, Y. Wang, S. Wang, K. Tao, L. Zhan, J. Xu, High signal-to-noise ratio, single-frequency 2 μm Brillouin fiber laser. Opt. Lett. **39**, 2626–2628 (2014)
77. L.S. Yan, X.S. Yao, Y. Shi, A.E. Willner, Simultaneous monitoring of both optical signal-to-noise ratio and polarization-mode dispersion using polarization scrambling and polarization beam splitting. J. Lightwave Technol. **23**, 3290 (2005)
78. D. Kouznetsov, J. Bisson, A. Shirakawa, K. Ueda, Limits of coherent addition of lasers: simple estimate. Opt. Rev. **12**, 445–447 (2005)
79. W. Chang, T. Wu, H. Winful, A. Galvanauskas, Array size scalability of passively coherently phased fiber laser arrays. Opt. Exp. **18**, 9634–9642 (2010)
80. S. Sivaramakrishnan, W. Chang, A. Galvanauskas, H.G. Winful, Dynamics of passively phased ring oscillator fiber laser arrays. IEEE J. Quant. Electron. **51**, 1–9 (2015)
81. E.J. Bochove, S.A. Shakir, Analysis of a spatial-filtering passive fiber laser beam combining system. IEEE J. Sel. Top. Quant. Electron. **15**(320–327), 78 (2009)
82. S. Barua, N. Das, S. Nordholm, M. Razaghi, Comparison of pulse propagation and gain saturation characteristics among different input pulse shapes in semiconductor optical amplifiers. Opt. Commun. **359**, 73–78 (2016)